[CANCER RESEARCH 64, 6259–6265, September 1, 2004]

Visualization of Intrathoracically Disseminated Solid Tumors in Mice with Optical Imaging by Telomerase-Specific Amplification of a Transferred Green Fluorescent Protein Gene

Tatsuo Umeoka,[1] Takeshi Kawashima,[1] Shunsuke Kagawa,[1,2] Fuminori Teraishi,[1] Masaki Taki,[1] Masahiko Nishizaki,[1] Satoru Kyo,[3] Katsuyuki Nagai,[4] Yasuo Urata,[4] Noriaki Tanaka,[1] and Toshiyoshi Fujiwara[1,2]

[1]Division of Surgical Oncology, Department of Surgery, Okayama University Graduate School of Medicine and Dentistry, Okayama, Japan; [2]Center for Gene and Cell Therapy, Okayama University Hospital, Okayama, Japan; [3]Department of Obstetrics and Gynecology, Kanazawa University School of Medicine, Kanazawa, Japan; and [4]Oncolys BioPharma, Inc., Tokyo, Japan

ABSTRACT

Currently available methods for detection of tumors *in vivo* such as X-ray, computed tomography, and ultrasonography are noninvasive and have been well studied; the images, however, are not specific for tumors. Direct optical imaging of tumor cells *in vivo* that can clearly distinguish them from surrounding normal tissues may be clinically useful. Here, we describe a new approach to visualizing tumors whose fluorescence can be detected using tumor-specific replication-competent adenovirus (OBP-301, Telomelysin) in combination with Ad-*GFP*, a replication-deficient adenovirus expressing green fluorescent protein (GFP). Human telomerase reverse transcriptase is the catalytic subunit of telomerase, which is highly active in cancer cells but quiescent in most normal somatic cells. We constructed an adenovirus 5 vector in which the human telomerase reverse transcriptase promoter element drives expression of *E1A* and *E1B* genes linked with an internal ribosome entry site and showed that OBP-301 replicated efficiently in human cancer cells, but not in normal cells such as human fibroblasts. When the human lung and colon cancer cell lines were infected with Ad-*GFP* at a low multiplicity of infection, GFP expression could not be detected under a fluorescence microscope; in the presence of OBP-301, however, Ad-*GFP* replicated in these tumor cells and showed strong green signals. In contrast, coinfection with OBP-301 and Ad-*GFP* did not show any signals in normal cells such as fibroblasts and vascular endothelial cells. We also found that established subcutaneous tumors could be visualized after intratumoral injection of OBP-301 and Ad-*GFP*. A549 human lung tumors and SW620 human colon tumors transplanted into BALB/c *nu/nu* mice were intratumorally injected with 8×10^5 plaque-forming units of Ad-*GFP* in combination with 8×10^6 plaque-forming units of OBP-301. Within 3 days of treatment, the fluorescence of the expressed GFP became visible by a three-chip color cooled charged-coupled device camera in these tumors, whereas intratumoral injection of Ad-*GFP* alone could not induce GFP fluorescence. Moreover, intrathoracic administration of Ad-*GFP* and OBP-301 could visualize disseminated A549 tumor nodules in mice after intrathoracic implantation. Our results indicate that intratumoral or intrathoracic injection of Ad-*GFP* in combination with OBP-301 might be a useful diagnostic method that provides a foundation for future clinical application.

INTRODUCTION

A variety of imaging technologies are being investigated as tools for cancer diagnosis, detection, and treatment monitoring. Improvements in methods of external imaging such as computed tomography, magnetic resonance imaging, and ultrasound techniques have increased the sensitivity for visualizing tumors and metastases (1, 2); a limiting factor in structural and anatomical imaging, however, is the inability to specifically identify malignant tissues. Histopathological examination is still the most effective method for the detection of neoplastic lesions. Thus, tumor-specific imaging would be of considerable value in treatment of human cancer by defining the location and area of tumors without microscopic analysis. In particular, if tumors too small for direct visual detection and therefore not detectable by direct inspection could be imaged *in situ*, surgeons could precisely excise tumors with appropriate surgical margins. This paradigm requires an appropriate marker that can facilitate visualization of physiological or molecular events that occur in tumor cells but not normal cells.

Molecular and functional monitoring of cellular processes has become a reality with the development of the green fluorescent protein (GFP) technology, which was originally identified from the jellyfish *Aequorea victoria* (3–5). GFP is able to specifically label biological molecules and cellular structures and can be sensitively detected by a variety of optical techniques. These labels can be detected in living tissues because of the relatively noninvasive nature of fluorescence, thus allowing transient and dynamic events to be visualized and measured (6–10). In addition, because GFP is genetically encoded, cells can be labeled by introducing the exogenous *GFP* gene. Indeed, Yang *et al.* (11) have shown that GFP-expressing tumors growing and metastasizing in intact animals could be viewed externally with a whole-body optical imaging system. Moreover, transgene expression could also be monitored by using an adenovirus vector expressing the *GFP* gene. These observations indicate that the GFP-based approach might be feasible as well as practical for real-time tumor imaging in living mammalians.

To specifically distinguish tumors from normal tissues, an appropriate strategy to make tumor cells selectively fluorescent is required. We previously constructed the tumor-specific replication-selective adenovirus OBP-301 (Telomelysin), in which the human telomerase reverse transcriptase (hTERT) promoter element drives expression of the *E1A* and *E1B* genes linked with an internal ribosome entry site, and demonstrated the selective replication and antitumor effect of OBP-301 in human cancer cells *in vitro* and *in vivo* (12). Because >85% of human cancer cells (but not most somatic normal cells) display telomerase activity (13, 14), we hypothesized that OBP-301 infection could complement *E1* gene functions and selectively facilitate replication of E1-deleted replication-deficient vectors in coinfected tumor cells.

In the present study, using a replication-deficient adenovirus expressing the *GFP* gene in combination with OBP-301, we demonstrate a real-time fluorescence optical imaging of pleural dissemination of human non–small-cell lung cancer cells in an orthotopic murine model. This novel molecular imaging technique could be feasible for *in vivo* detection of disseminated small tumor nodules.

MATERIALS AND METHODS

Cells and Culture Conditions. The human non–small-cell lung cancer cell lines H1299, H358, and H226Br and the human colorectal carcinoma cell lines

Received 4/15/04; revised 6/16/04; accepted 7/7/04.

Grant support: Grants from the Ministry of Education, Science, and Culture and the Ministry of Health and Welfare, Japan.

The costs of publication of this article were defrayed in part by the payment of page charges. This article must therefore be hereby marked *advertisement* in accordance with 18 U.S.C. Section 1734 solely to indicate this fact.

Requests for reprints: Toshiyoshi Fujiwara, Center for Gene and Cell Therapy, Okayama University Hospital, 2-5-1 Shikata-cho, Okayama 700-8558, Japan. E-mail: toshi_f@md.okayama-u.ac.jp.

SW620, LoVo, and DLD-1 were routinely propagated in monolayer culture in RPMI 1640 supplemented with 10% fetal calf serum (FCS). The human non–small-cell lung cancer cell line A549 was cultured in Dulbecco's modified Eagle's medium containing nutrient mixture (Ham's F-12). The transformed embryonic kidney cell line 293 was grown in Dulbecco's modified Eagle's medium containing high glucose (4.5 g/L) and supplemented with 10% FCS. The normal human lung diploid fibroblast cell line WI-38 (JCRB0518) was obtained from the Health Science Research Resources Bank (Osaka, Japan) and grown in Eagle's minimal essential medium with 10% FCS. The normal human lung fibroblast cell line NHLF was purchased from TaKaRa Biomedicals (Kyoto, Japan) and cultured in the medium recommended by the manufacturer. The human umbilical vascular endothelial cell line HUVEC was kindly provided by Dr. Masayoshi Namba (Okayama University, Okayama, Japan) and propagated in monolayer culture in CSC certified medium with 100 units/ml penicillin and 100 mg/ml streptomycin.

Recombinant Adenoviruses. The recombinant replication-selective, tumor-specific adenovirus vector was constructed and characterized previously (12). The resultant virus was named OBP-301. The adenoviral vector containing GFP cDNA (Ad-*GFP*) was also used. Viral stocks were quantified by a plaque-forming assay using 293 cells and stored at −80°C.

Quantitative Real-Time Polymerase Chain Reaction Analysis. Total RNA from the tumor samples and cultured cells was obtained using the RNeasy Mini Kit (Qiagen, Chatsworth, CA). Approximately 0.1 μg of total RNA was used for reverse transcription. Reverse transcription was performed at 22°C for 10 minutes and then at 42°C for 20 minutes. The *hTERT* mRNA copy number was determined by real-time quantitative reverse transcription-polymerase chain reaction (RT-PCR) using a LightCycler instrument and a LightCycler DNA TeloTAGGG Kit (Roche Molecular Biochemicals, Indianapolis, IN). Polymerase chain reaction amplification began with a 60-second denaturation step at 95°C, followed by 40 cycles of denaturation at 95°C for 15 seconds, annealing at 58°C for 10 seconds, and extension at 72°C for 9 seconds.

Fluorescent Microscopy. Human cancer cells (SW620, A549, and H1299) and normal cells (WI-38, NHLF, and HUVEC) were infected with 0.1 multiplicity of infection (MOI) of Ad-*GFP* alone or in combination with 1 MOI of OBP-301 *in vitro*. Expression of the *GFP* gene was assessed and photographed (×200) by an Eclipse TS-100 fluorescent microscope (Nikon, Tokyo, Japan) 24 hours after infection.

Animal Experiments. The experimental protocol was approved by the Ethics Review Committee for Animal Experimentation of Okayama University (Okayama, Japan). SW620 and A549 xenografts were produced on the back of 5-week-old female BALB/c *nu/nu* mice by subcutaneous injection of 5×10^6 SW620 or A549 cells in 500 μl of Hanks' balanced salt solution. Three weeks after tumor cell inoculation, both tumors received intratumoral injection with Ad-*GFP* [8×10^5 plaque-forming units (pfu)/50 μl] alone or Ad-*GFP* (8×10^5 pfu/25 μl) plus OBP-301 (8×10^6 pfu/25 μl). Mice were anesthetized by intraperitoneal injection of pentobarbital (50 mg/kg) on days 1, 2, 3, 7, and 14 after virus injection and examined for GFP expression. As a control, viruses were subcutaneously injected into non–tumor-bearing mice. To generate an orthotopic model of pleural dissemination, female BALB/c *nu/nu* mice received intrathoracic injection with a cell suspension of A549 cells at a density of 5×10^6 cells/200 μl through a 27-gauge needle. Two weeks later, Ad-*GFP* (4×10^7 pfu/50 μl) and OBP-301 (4×10^7 pfu/50 μl) were injected into the thoracic space by the same technique. Five days after virus injection, mice were sacrificed, and their thoracic spaces were examined.

Cooled Charged-Coupled Device Imaging. *In vivo* GFP fluorescence imaging was acquired by illuminating the animal with a Xenon 150-W lamp. The re-emitted fluorescence was collected through a long pass filter on a Hamamatsu C5810 three-chip color cooled charged-coupled device (CCD) camera (Hamamatsu Photonics Systems, Hamamatsu, Japan). High-resolution image acquisition was accomplished using an EPSON personal computer. Images were processed for contrast and brightness with the use of Adobe Photoshop 4.0.1J software.

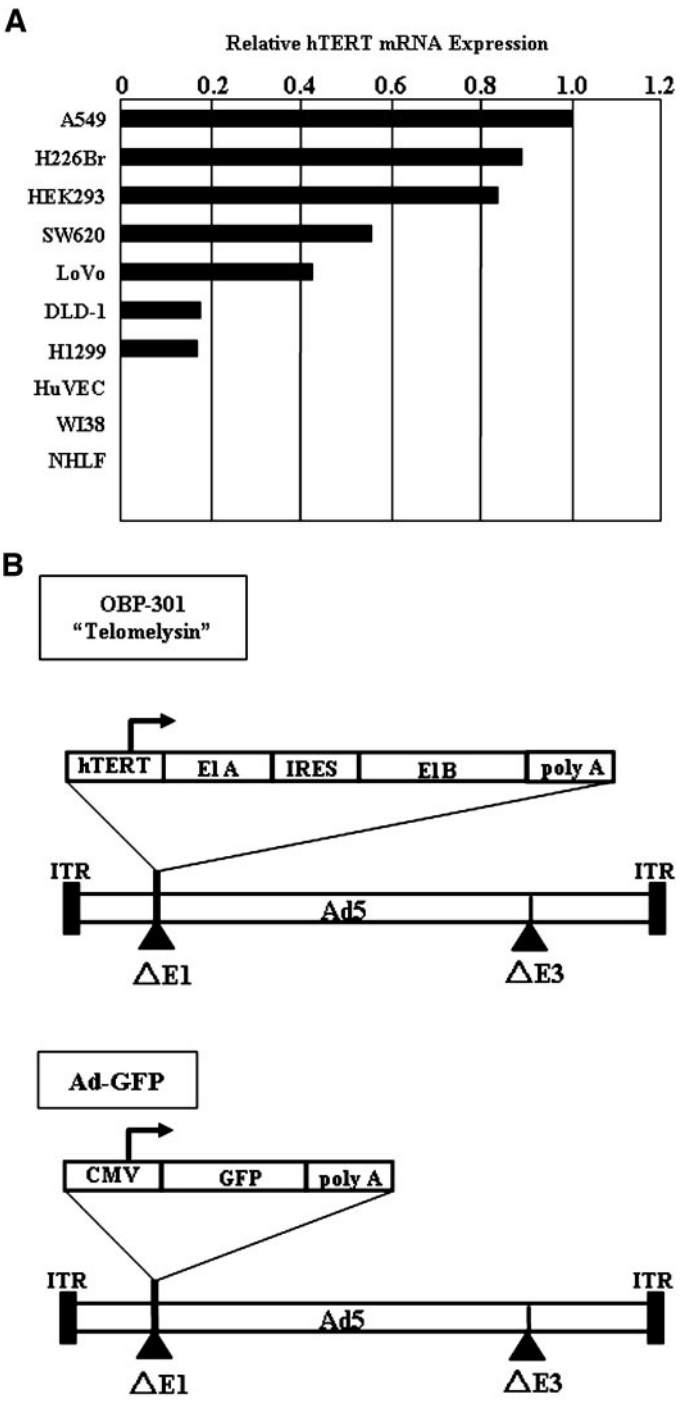

Fig. 1. *A*, relative *hTERT* mRNA expression in human tumor and normal cells determined by real-time RT-PCR analysis. The *hTERT* mRNA expression of A549 human lung cancer cells was considered to be 1.0, and the relative expression level of each cell line was calculated against that of A549 cells. *B*, schematic DNA structures of OBP-301 and Ad-*GFP*. OBP-301 contains the hTERT promoter sequence inserted into the E3-deleted adenovirus genome to drive transcription of the E1A and E1B bicistronic cassette linked by the internal ribosome entry site structure. The Ad-*GFP* vector contains GFP cDNA driven by the cytomegalovirus promoter.

RESULTS

Human Telomerase Reverse Transcriptase Levels in Human Cancer and Normal Cells. Telomerase is a novel marker for malignant diseases (15). To confirm the specificity of telomerase activity in human cancer cells, expression of *hTERT* mRNA, which plays a key role in telomerase activation (16), was measured in a panel of human tumor and normal cell lines using a real-time RT-PCR method. All tumor cell lines, including human non–small-cell lung cancer cell lines A549, H226Br, and H1299 and human colorectal cancer cell lines SW620, LoVo, and DLD-1, expressed detectable levels of *hTERT* mRNA, although the levels of expression varied widely (Fig.

1*A*). In contrast, human fibroblast cells such as WI-38 and NHLF were negative for hTERT expression. HUVEC cells transformed with the SV40 large T-antigen gene also exhibited no *hTERT* mRNA expression. 293 cells are known to be telomerase positive and were used as a positive control. These results suggest that the hTERT promoter element can be used to target human cancer.

Selective Visualization of Human Cancer Cells *In vitro*. To selectively enhance GFP transgene expression in human cancer cells, we used a tumor- or telomerase-specific replication-selective adenovirus, OBP-301, and replication-deficient Ad-*GFP*. Schematic DNA structures of OBP-301 and Ad-*GFP* are shown in Fig. 1*B*. SW620, A549, and H1299 human cancer cells expressed bright GFP fluorescence as early as 24 hours after coinfection with Ad-*GFP* (0.1 MOI) and OBP-301 (1.0 MOI) (Fig. 2). The fluorescence intensity increased gradually until approximately 3 days after infection, followed by rapid cell death due to the cytopathic effect of OBP-301 (data not shown). Inection with Ad-*GFP* alone at a MOI of 0.1 caused neither GFP expression nor cytotoxicity in SW620 and A549 cells. Only faint fluorescence could be detected in H1299 cells infected with 0.1 MOI of Ad-*GFP* because H1299 cells are highly sensitive to adenovirus infection. In contrast, normal human cells, including WI-38, NHLF, and HUVEC, were completely negative for GFP expression after coinfection with Ad-*GFP* and OBP-301. These results indicate that Ad-*GFP* can replicate exclusively in human cancer cells in the presence of OBP-301, leading to tumor cell-specific GFP fluorescence expression *in vitro*.

Dose-Dependent Intensity of Fluorescence by Ad-*GFP* Injection into Mice. To selectively detect tumor tissues *in vivo*, nonspecific *GFP* transgene expression in normal organs must be avoided. We first determined the optimal dose of Ad-*GFP* that could not induce detectable GFP fluorescence in normal tissues. Non–tumor-bearing mice received subcutaneous injection with increasing doses of Ad-*GFP* alone and were then monitored for fluorescence intensity over time with the CCD noninvasive imaging system. As shown in Fig. 3, mice given 1.3×10^9 and 1.3×10^8 pfu of Ad-*GFP* displayed high and moderate GFP fluorescence signals in the skin, respectively, within 24 hours after injection. In contrast, the *GFP* transgene expression was not visible over a 7-day period after injection of 1.3×10^7 or 1.3×10^6 pfu of Ad-*GFP*. Thus, 10^8 pfu was considered the lowest dose of Ad-*GFP* that induces nonspecific GFP signals in normal tissues.

Selective Visualization of Subcutaneously Growing Human Tumors *In vivo*. To further confirm the specificity of the GFP-based fluorescent optical detection of tumors *in vivo*, we performed a set of control experiments. In the control group of non–tumor-bearing animals that received subcutaneous injection with 8×10^5 pfu of Ad-*GFP* plus 8×10^6 pfu of OBP-301, no apparent GFP signals were detected in the skin over 7 consecutive days (Fig. 4*A*). Moreover, injection of Ad-*GFP* alone at a density of 8×10^5 pfu into subcutaneously established SW620 tumors resulted in no GFP fluorescence expression for at least 7 days after injection (Fig. 4*B*).

We next examined the kinetics of *GFP* transgene expression in

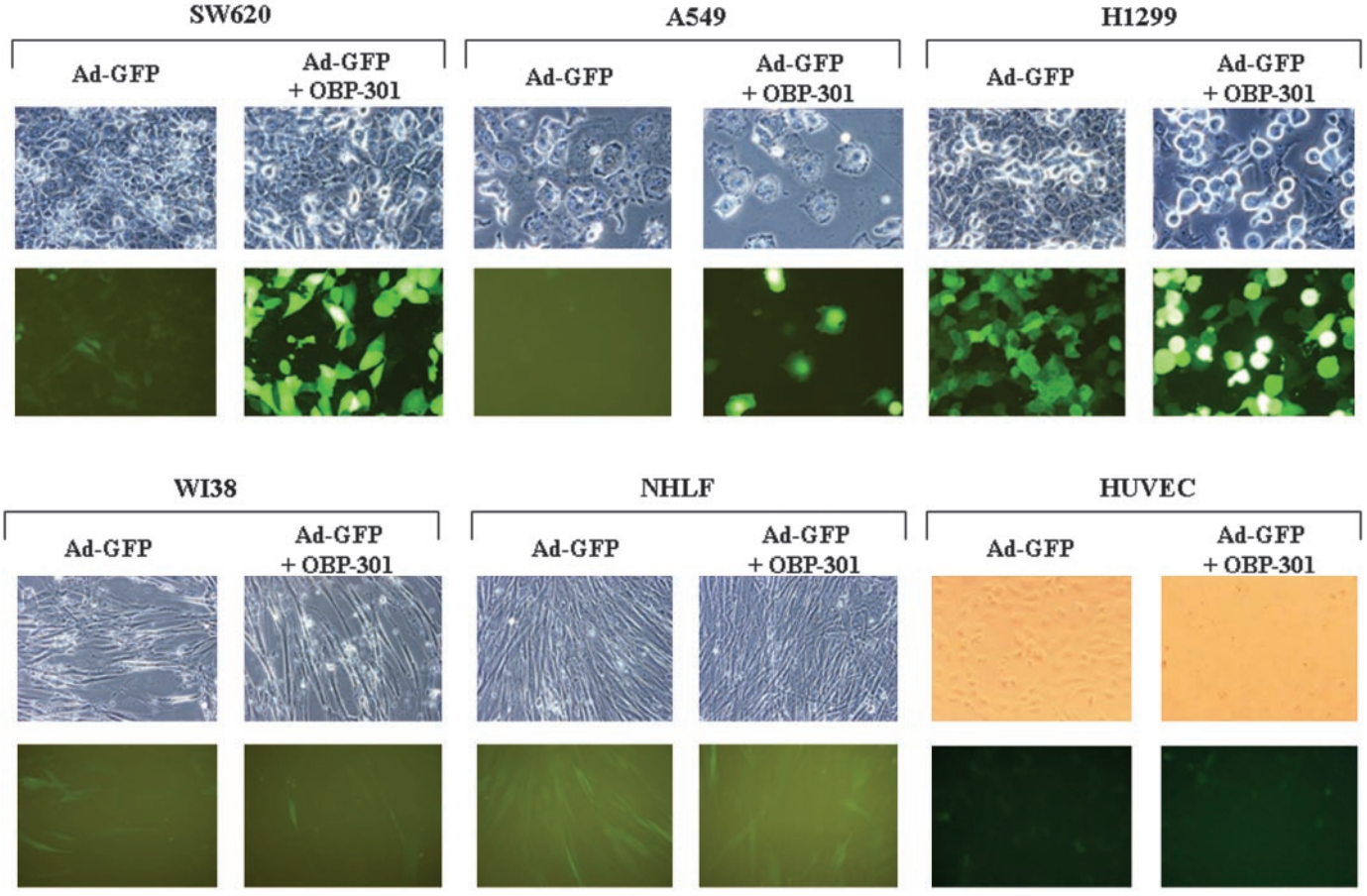

Fig. 2. Selective bystander replication of Ad-*GFP* in the presence of OBP-301 in human cancer cells *in vitro*. Cultured human cancer [SW620 (colorectum), A549 (lung), and H1299 (lung)] and normal cells (WI-38, NHLF, and HUVEC) were infected with 0.1 MOI of Ad-*GFP* alone or in combination with 1.0 MOI of OBP-301, and photographed under a fluorescence microscope for GFP expression 24 hours after treatment. Magnification, ×200.

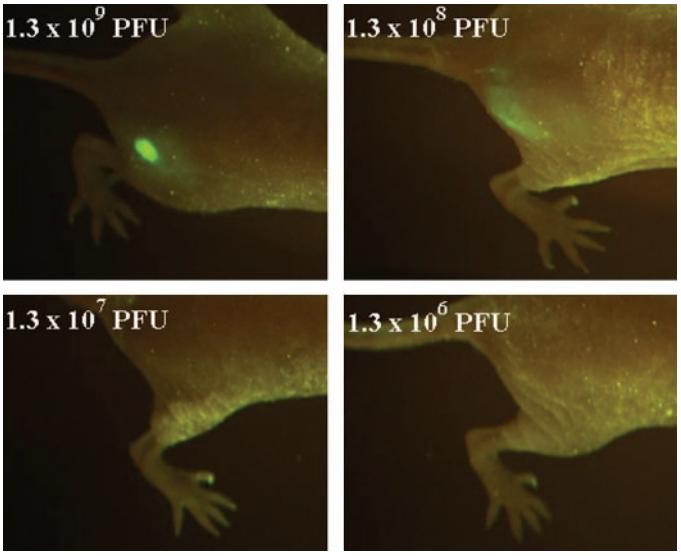

Fig. 3. External images of non–tumor-bearing *nu/nu* mice that received injection with increasing doses of Ad-*GFP* alone. Non–tumor-bearing mice received subcutaneous injection with 1.3×10^6, 1.3×10^7, 1.3×10^8, or 1.3×10^9 pfu of Ad-*GFP* alone and were photographed for GFP expression by the CCD noninvasive imaging system 24 hours after injection.

SW620 and A549 tumors after intratumoral injection of 8×10^5 pfu of Ad-*GFP* and 8×10^6 pfu of OBP-301. Treated mice displayed detectable intratumoral signals within 24 hours after local delivery of viruses (Fig. 5). Whole-body images of mice showed light spots in the tumor area, although complete tumor images were not observed. The fluorescence intensity reached maximum levels 3 to 7 days after injection and gradually decreased to background fluorescence by 14 days after treatment. When mice were sacrificed 7 days after intratumoral injection of viruses, GFP expression was confined to the tumor; no GFP fluorescence was detected in various normal organs such as the liver, kidney, spleen, small intestine, brain, heart, pancreas, ovary, and adrenal gland (data not shown).

Selective Visualization of Pleural Dissemination of Human Lung Cancer Cells *In vivo*. We also evaluated the potential of GFP-based visualization of A549 human non–small-cell lung cancer cells growing intrathoracically in athymic *nu*/*nu* mice. We reported previously (17) that when A549 cells were inoculated into the thoracic space, dissemination of tumors appeared in all mice 14 days after tumor injection. As shown in Fig. 6, the optical CCD imaging of the thoracic cavity after a midsternal thoracotomy demonstrated that disseminated tumor nodules in the visceral pleura, parietal pleura, diaphragmatic pleura, and mediastinum could be detected as light-emitting spots by intrathoracic coinjection of 4×10^7 pfu of Ad-*GFP* and 4×10^7 pfu of OBP-301. The large tumors were labeled in spots with GFP fluorescence; small nodules, however, could be imaged entirely as intensive GFP signals. Histological analysis confirmed the presence of disseminated tumor cells in the sites of fluorescence emission (Fig. 6). The thoracic cavity of non–tumor-bearing mice was negative for *GFP* transgene expression (data not shown).

DISCUSSION

Gene-based therapeutic strategies, including replacement of defective tumor suppressors, enhancement of immune-mediated tumor surveillance, and tumor-selective virotherapy, have emerged as promising adjuvants to conventional modalities for human cancer (18–21). We previously reported (12) the development of a tumor-specific replication-selective adenovirus, OBP-301, which is capable of replicating exclusively in telomerase-positive human cancer cells. In the current study, we investigated the potential of OBP-301 to visualize human tumors by facilitating replication of a GFP-expressing replication-deficient adenovirus, Ad-*GFP*. As reported previously (8), for real-time imaging of growing tumors in live mice, GFP appears to be an extremely effective tumor cell marker to identify tumor tissues at

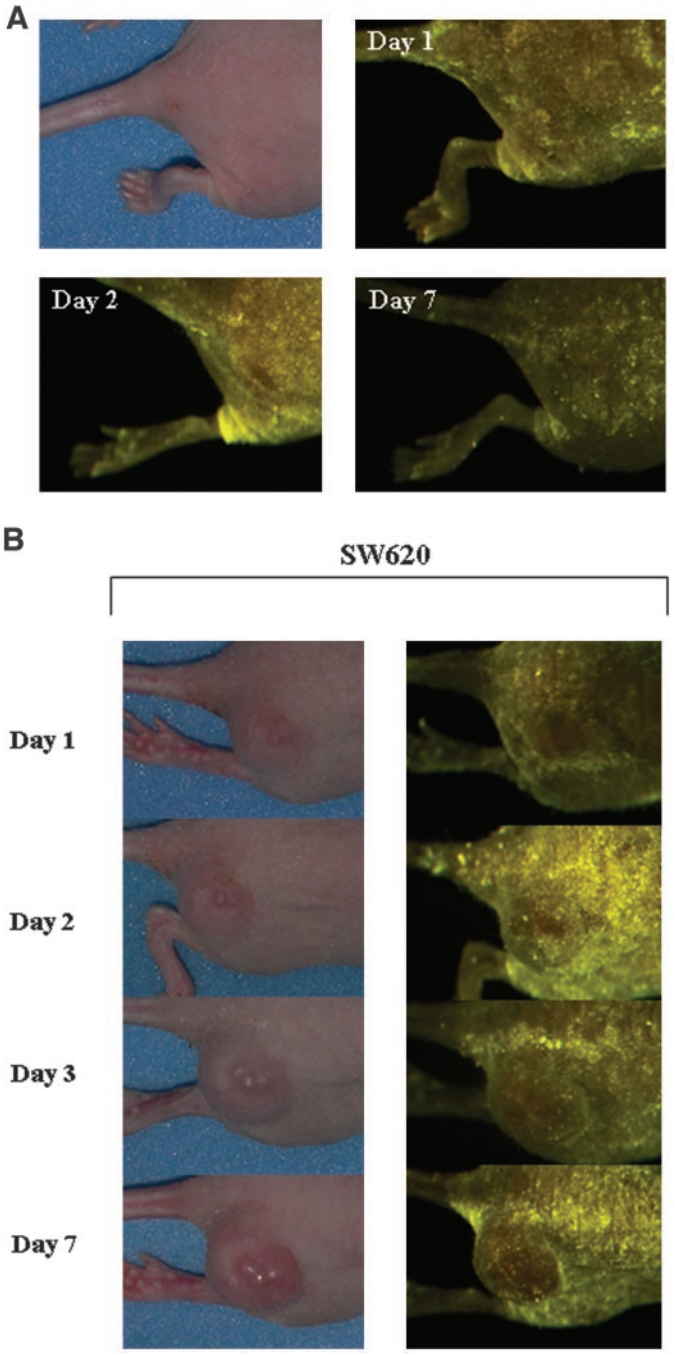

Fig. 4. *A*, external images of non–tumor-bearing mice that received injected with Ad-*GFP* plus OBP-301. As a control, non–tumor-bearing mice received subcutaneous injection with 8×10^5 pfu of Ad-*GFP* in combination with 8×10^6 pfu of OBP-301 and were assessed for GFP fluorescence 24 hours after administration. As expected, no GFP signals were obtained. *Top left panel*, macroscopic appearance of mouse. *B*, external images of SW620 tumor-bearing *nu/nu* mice that received injection with Ad-*GFP* alone. Three weeks after subcutaneous inoculation of SW620 tumor cells (5×10^6 cells/mouse), mice received intratumoral injection of Ad-*GFP* at a density of 8×10^5 pfu alone. As expected, no GFP fluorescence expression was detected for at least 7 days after injection. *Left panels*, macroscopic appearance of SW620 tumors; *right panels*, fluorescence detection.

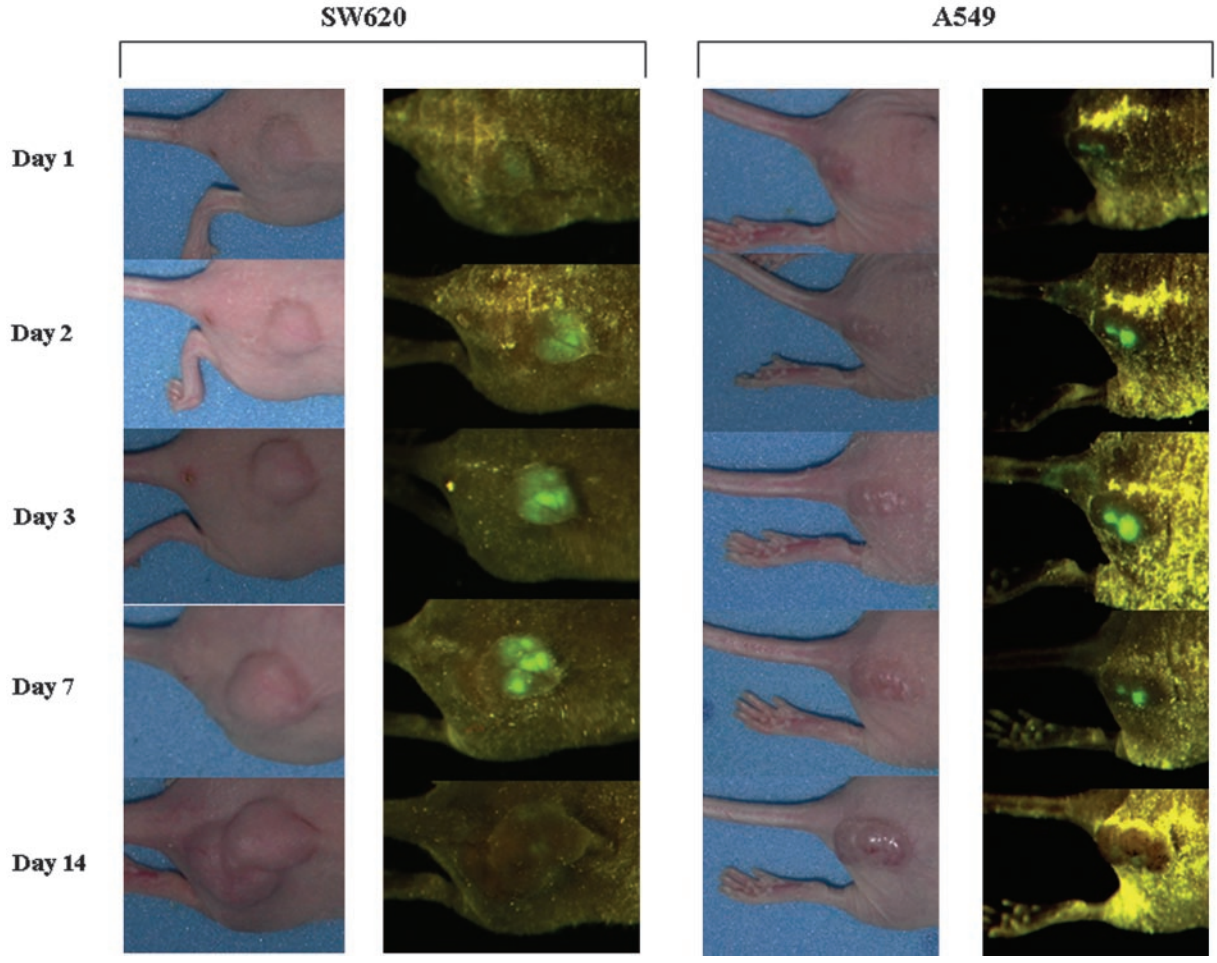

Fig. 5. Time course of external images of subcutaneous SW620 and A549 tumors after intratumoral injection of Ad-*GFP* plus OBP-301. Three weeks after subcutaneous inoculation of SW620 and A549 tumor cells (5×10^6 cells/mouse), Ad-*GFP* and OBP-301 at concentrations of 8×10^5 pfu and 8×10^6 pfu, respectively, were injected directly into established tumors. The GFP fluorescence intensity was monitored for 14 consecutive days under the CCD noninvasive imaging system. *Left panels*, macroscopic appearance of subcutaneous tumors; *right panels*, fluorescence detection.

a single-cell level. A major advantage of GFP labeling is that it requires no preparative procedures such as contrast agents, substrates, and light-tight boxes, unlike other imaging techniques.

Elevated levels of telomerase activity are found in the majority of malignancies (Fig. 1*A*) and believed to play a critical role in tumorigenesis (22). Therefore, telomerase-specific OBP-301 was able to selectively compensate the *E1* gene products for Ad-*GFP* that lacks E1 proteins in human tumor cells, but not in normal cells. However, because the recombinant adenovirus vectors can efficiently infect a wide variety of dividing and nondividing cells and transfer exogenous genes into mammalian cells, infection with Ad-*GFP* alone at high concentrations may induce GFP fluorescence nonselectively in both tumor and normal cells. Our preliminary experiments demonstrated that infection with Ad-*GFP* alone at <1.0 MOI was insufficient to induce GFP expression under fluorescence microscopy in most tumor and normal cells *in vitro* (data not shown). We confirmed that coinfection with 0.1 MOI of Ad-*GFP* and 1.0 MOI of OBP-301 could express GFP fluorescence selectively in tumor cells, although detectable green signals were evident with Ad-*GFP* infection alone in cells sensitive to adenovirus infection, such as H1299 cells (Fig. 2). However, the fact that most normal cells are relatively resistant to adenovirus infection suggests that the false-positive detection of normal cells is likely to be less frequent.

It has been reported that 1.6×10^9 pfu of Ad-*GFP* delivered to various organs induced high-intensity GFP expression that could be visualized by whole-body imaging (11); therefore, we determined 10^7 pfu of Ad-*GFP* as a suboptimal dose for GFP detection *in vivo* by the dose titration study (Fig. 3). Indeed, intratumoral injection of 8×10^5 pfu of Ad-*GFP* plus 8×10^6 pfu of OBP-301 resulted in intense GFP expression in tumors, whereas no GFP signals were detectable by subcutaneous administration of these vectors into normal areas (Figs. 4 and 5). CCD imaging demonstrated the heterogeneous pattern of GFP expression only in tumors in mice that received intratumoral injection of 50 μl of the vector solution, suggesting that the vectors might not be able to spread throughout the tumor tissues (Fig. 5). Moreover, the green signals in tumors disappeared within 14 days after intratumoral injection of Ad-*GFP* and OBP-301, presumably on dilution of the vectors with tumor cell proliferation (Fig. 5). We showed previously (12) that intratumoral injection of OBP-301 was effective for suppressing the growth of H1299 human lung tumors subcutaneously transplanted into *nu/nu* mice; 8×10^6 pfu of OBP-301, however, might be insufficient for growth inhibition of SW620 and A549 tumors. Additional studies are required to determine the optimal doses of vectors to obtain complete and prolonged GFP labeling of solid tumors.

Progression of non–small-cell lung cancer is characterized by the dissemination of malignant pulmonary epithelial cells (23). To overcome the poor prognosis of lung cancer involving the pleura, innovative methodology for early diagnosis as well as treatment is needed. We reported previously (17) that intrathoracic injection of replication-

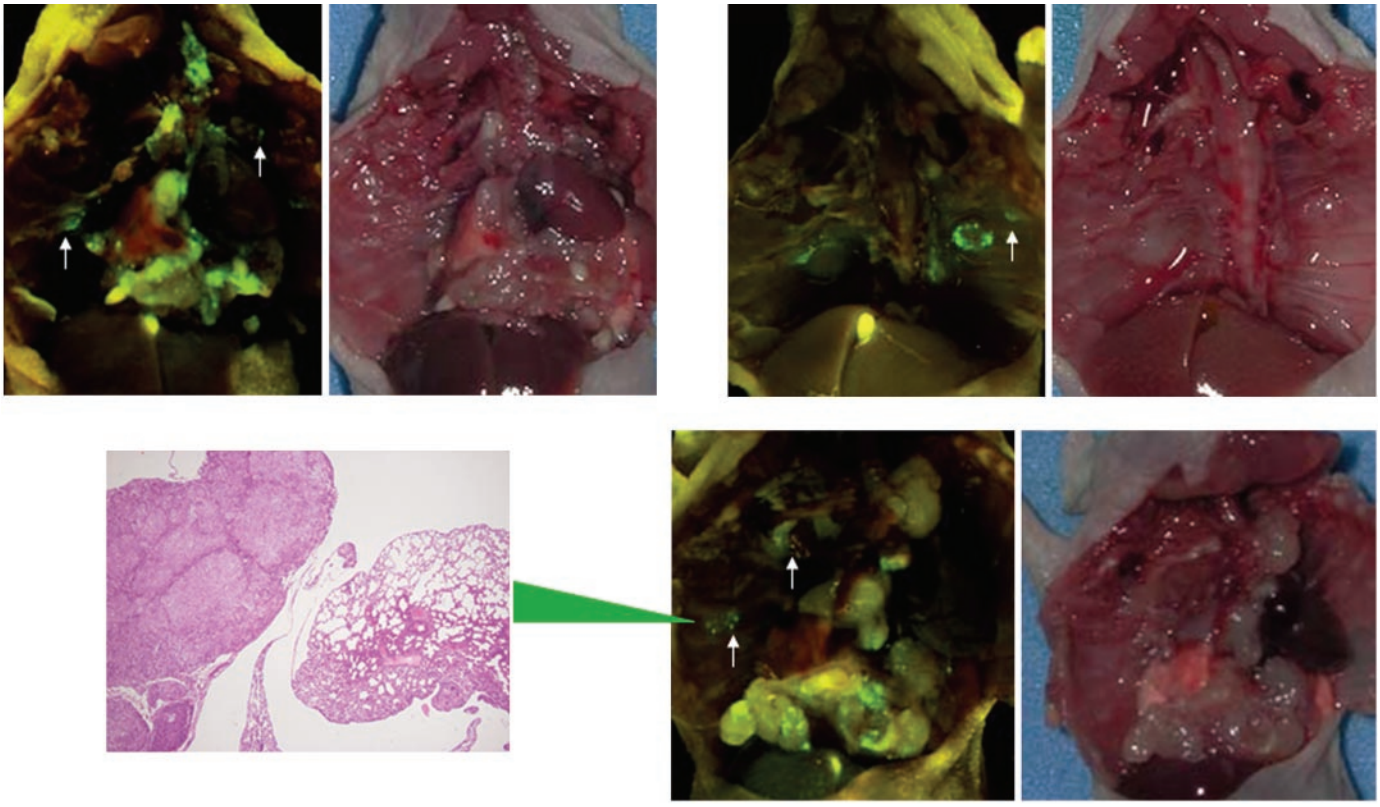

Fig. 6. Internal images of pleural dissemination visualized by intrathoracic injection of Ad-*GFP* and OBP-301. Female BALB/c *nu*/*nu* mice received intrathoracic implant with 5×10^6 A549 tumor cells. Two weeks later, 4×10^7 pfu/50 μl each of Ad-*GFP* and OBP-301 were injected into the thoracic space. Five days after virus injection, mice were sacrificed, and their thoracic spaces were examined. Three representative mice are shown. *Left panels*, fluorescent detection; *right panels*, gross appearance of A549 tumors grown orthotopically in the thoracic spaces. *Arrows*, disseminated tiny tumor. *Bottom left panel*, H&E staining of the lesion of fluorescence emission. Magnification, ×100.

deficient adenovirus expressing antisense against heparanase, which is associated with metastatic potential, inhibited pleural dissemination of human lung cancer cells in an orthotopic murine model. These observations suggest that intrathoracically administered adenovirus is capable of infecting disseminated neoplastic nodules in the thoracic cavity. Obstacles to effective diagnosis and therapy for pleural dissemination include the fact that tumors that are either too small or hidden in an internal body location could not be visually detected. Our optical CCD imaging was able to visualize tiny foci of pleural dissemination of A549 human lung cancer cells with GFP fluorescence after intrathoracic injection of OBP-301 and Ad-*GFP*, although these lesions could not be macroscopically identified (Fig. 6). Several studies have demonstrated the utility of CCD imaging to track metastasis and/or dissemination of tumor cells that were stably transfected with the *GFP* gene in small animals (6–10); the vector-based strategy in the present study, however, is considered more convenient and clinically relevant. If target lesions can be identified during thoracotomy, surgeons will be capable of removing disseminated tumors. Moreover, a future option may be to develop robotic laser therapy for pleural dissemination with an automatic detection tool that chases GFP fluorescence under thoracoscopy.

The approach is considered to be promising; however, it also suffers from some limitations. For example, tumors existing within organs could not be detected because detection requires exposing the tumors to a Xenon lamp. Because the entire tumors were not fluorescent (except for very tiny tumors), the margins of invasive tumors that are not clearly encapsulated might go unseen. In addition, the distant metastatic tumors could not be visualized by intratumorally or regionally injected OBP-301 and Ad-*GFP*. As a means to circumvent this limitation, development of the tumor-specific replication-selective adenovirus OBP-401, in which the *GFP* gene was inserted, has allowed systemic administration, leading to the whole-body distribution of the vector, thereby detecting distant metastatic lesions with telomerase-specific GFP expression. Preclinical studies using OBP-401 are currently under way in our laboratory.

In conclusion, our data presented here indicate that locoregional injection of Ad-*GFP* plus OBP-301 in combination with highly sensitive CCD imaging might be a useful diagnostic strategy for real-time visualization of macroscopically invisible tumor tissues. Although the sensitivity and specificity of the method must be assessed by additional experiments, this technology provides a foundation for future clinical application.

REFERENCES

1. Tearney GJ, Brezinski ME, Bouma BE, et al. In vivo endoscopic optical biopsy with optical coherence tomography. Science (Wash DC) 1997;276:2037–9.
2. MacDonald SL, Hansell DM. Staging of non-small cell lung cancer: imaging of intrathoracic disease. Eur J Radiol 2003;45:18–30.
3. Misteli T, Spector DL. Applications of the green fluorescent protein in cell biology and biotechnology. Nat Biotechnol 1997;15:961–4.
4. van Roessel P, Brand AH. Imaging into the future: visualizing gene expression and protein interactions with fluorescent proteins. Nat Cell Biol 2002;4:E15–20.
5. Ehrhardt D. GFP technology for live cell imaging. Curr Opin Plant Biol 2003;6: 622–8.
6. Rashidi B, Yang M, Jiang P, et al. A highly metastatic Lewis lung carcinoma orthotopic green fluorescent protein model. Clin Exp Metastasis 2000;18:57–60.
7. Yang M, Baranov E, Jiang P, et al. Whole-body optical imaging of green fluorescent protein-expressing tumors and metastases. Proc Natl Acad Sci USA 2000;97:1206–11.
8. Hoffman RM. Visualization of GFP-expressing tumors and metastasis in vivo. Biotechniques 2001;30:1016–22, 1024–6.
9. Bouvet M, Wang J, Nardin SR, et al. Real-time optical imaging of primary tumor growth and multiple metastatic events in a pancreatic cancer orthotopic model. Cancer Res 2002;62:1534–40.

10. Yamamoto N, Yang M, Jiang P, et al. Real-time GFP imaging of spontaneous HT-1080 fibrosarcoma lung metastases. Clin Exp Metastasis 2003;20:181–5.
11. Yang M, Baranov E, Moossa AR, Penman S, Hoffman RM. Visualizing gene expression by whole-body fluorescence imaging. Proc Natl Acad Sci USA 2000;97: 12278–82.
12. Kawashima T, Kagawa S, Kobayashi N, et al. Telomerase-specific replication-selective virotherapy for human cancer. Clin Cancer Res 2004;10:285–92.
13. Kim NW, Piatyszek MA, Prowse KR, et al. Specific association of human telomerase activity with immortal cells and cancer. Science (Wash DC) 1994;266:2011–5.
14. Shay JW, Wright WE. Telomerase activity in human cancer. Curr Opin Oncol 1996;8:66–71.
15. Shay JW, Wright WE. Telomerase: a target for cancer therapeutics. Cancer Cell 2002;2:257–65.
16. Nakayama J, Tahara H, Tahara E, et al. Telomerase activation by hTRT in human normal fibroblasts and hepatocellular carcinomas. Nat Genet 1998;18:65–8.
17. Uno F, Fujiwara T, Takata Y, et al. Antisense-mediated suppression of human heparanase gene expression inhibits pleural dissemination of human cancer cells. Cancer Res 2001;61:7855–60.
18. Shao J, Fujiwara T, Kadowaki Y, et al. Overexpression of the wild-type p53 gene inhibits NF-kB activity and synergizes with aspirin to induce apoptosis in human colon cancer cells. Oncogene 2000;19:726–36.
19. Waku T, Fujiwara T, Shao J, et al. Contribution of CD95 ligand-induced neutrophil infiltration to the bystander effect in p53 gene therapy for human cancer. J Immunol 2000;165:5884–90.
20. Itoshima T, Fujiwara T, Waku T, et al. Induction of apoptosis in human esophageal cancer cells by sequential transfer of the wild-type p53 and E2F-1 genes: involvement of p53 accumulation via ARF-mediated MDM2 down-regulation. Clin Cancer Res 2000;6:2851–9.
21. Ohtani S, Kagawa S, Tango Y, et al. Quantitative analysis of p53-targeted gene expression and visualization of p53 transcriptional activity following intratumoral administration of adenoviral p53 in vivo. Mol Cancer Ther 2004;3:93–100.
22. Masutomi K, Hahn WC. Telomerase and tumorigenesis. Cancer Lett 2003;194:163–72.
23. Fukuse T, Hirata T, Tanaka F, Wada H. The prognostic significance of malignant pleural effusion at the time of thoracotomy in patients with non-small cell lung cancer. Lung Cancer 2001;34:75–81.